Analyst

Cite this: *Analyst*, 2012, **137**, 3076

www.rsc.org/analyst

PAPER

Convergence of Dip-Pen Nanolithography and acoustic biosensors towards a rapid-analysis multi-sample microsystem

Konstantinos Mitsakakis,*[ab] Sylwia Sekula-Neuner,[c] Steven Lenhert,[cde] Harald Fuchs[ce] and Electra Gizeli*[f]

Received 3rd February 2012, Accepted 19th April 2012
DOI: 10.1039/c2an35156k

The present work demonstrates for the first time patterning of a ready-to-use biosensor with several different biomolecules using Dip-Pen Nanolithography (DPN) for the development of a procedure towards more rapid and efficient multi-sample detection. The biosensor platform used is based on a Surface Acoustic Wave (SAW) device integrated with a parallel-channel microfluidic module, termed as "microfluidics-on-SAW" ("μF-on-SAW"), for reproducible multi-sample analysis. Lipids with different functionalized head groups were patterned at distinct, microfluidic-formed rectangular domains with sharp edges all located on the same sensor surface; pattern quality was verified using a fluorescent microscope. The functionality of the head groups, the efficiency of the patterning method, and the suitability of DPN for the surface modification of the acoustic device were subsequently examined through acoustic experiments. The μF-on-SAW configuration was used to detect specific binding between the pre-patterned functionalized lipids with their corresponding biomolecules. The achievement of an improved sensitivity (5-fold compared to previous acoustic configurations) and reduced preparation time by at least 2 h clearly indicates the suitability of DPN as a direct patterning method for ready-to-use acoustic sensor devices like the μF-on-SAW towards integrated, rapid-analysis, multi-sample biosensing microsystem development.

Introduction

Well-established biosensor technologies, irrespective of their detection principle, are gradually evolving from single- to multi-sample platforms providing benefits to a vast range of application fields such as cancer diagnostics, biomarker detection (*e.g.*, cardiac markers for early assessment of cardiovascular risk), early-stage identification of genetic anomalies, high throughput analysis of new drugs and investigation of emerging biomarkers.[1–3] In this direction, acoustic sensors follow the multi-analyte trend with a recently emerged concept based on microfluidics. Contrary to the traditional approach, according to which Surface Acoustic Wave (SAW) or Quartz Crystal Microbalance (QCM) sensing elements are placed one next to the other to form an array,[4–6] the "microfluidics-on-SAW" ("μF-on-SAW") concept utilizes a series of parallel microfluidic channels in order to compartmentalize the total surface of a single sensor (standard configuration) into discrete domains, each hosting an individual experiment (Fig. 1(a)).[7,8] Advantages of this setup over classic SAW sensor arrays are: (i) cross-domain reproducibility as high as 90%, (ii) utilization of the same measurement instrumentation used for the standard configuration, and (iii) versatility in the number of tested samples, since three-, four-, or five-channel modules are interchangeable, depending on the number of desired analytes. A series of applications have demonstrated the reliability of this setup in multi-sample sensing in protein detection[9] and cardiovascular risk assessment.[10]

Typical experimental protocols followed in biosensors impose some *in situ* steps prior to the detection of the actual analyte, mainly for the immobilization of a specific receptor, *e.g.*, streptavidin/NeutrAvidin, or protein G adsorption for subsequent binding of biotinylated molecules or antibodies, respectively. As they are a part of the actual experimental procedure, these steps inevitably increase the overall analysis time, cost, and sample consumption, an effect that is maximized when multiplicity is considered.

Applying *ex situ* biomolecule patterning as a biochip preparation process is a promising means to overcome the aforementioned drawbacks and render the entire detection procedure more automated, shortening the required time and promoting

[a]*Institute of Molecular Biology & Biotechnology, Foundation for Research & Technology Hellas, 100 N. Plastira Street, Heraklion Crete, GR-700 13, Greece. E-mail: kmits@imbb.forth.gr; Fax: +30 2810 394408; Tel: +30 2810 394373*
[b]*Department of Materials Science & Technology, University of Crete, Vassilika Vouton, Heraklion, GR-710 03, Greece*
[c]*Institute of Nanotechnology, Karlsruhe Institute of Technology, Karlsruhe Nano Micro Facility (KNMF), D-76021 Karlsruhe, Germany*
[d]*Department of Biological Science and Integrative NanoScience Institute, Florida State University, Tallahassee, Florida 32306-4370, USA*
[e]*Physikalisches Institut, Universität Münster, and Center for Nanotechnology (CeNTech), D-48149 Münster, Germany*
[f]*Department of Biology, University of Crete, Vassilika Vouton, Heraklion, GR-714 09, Greece. E-mail: gizeli@imbb.forth.gr*

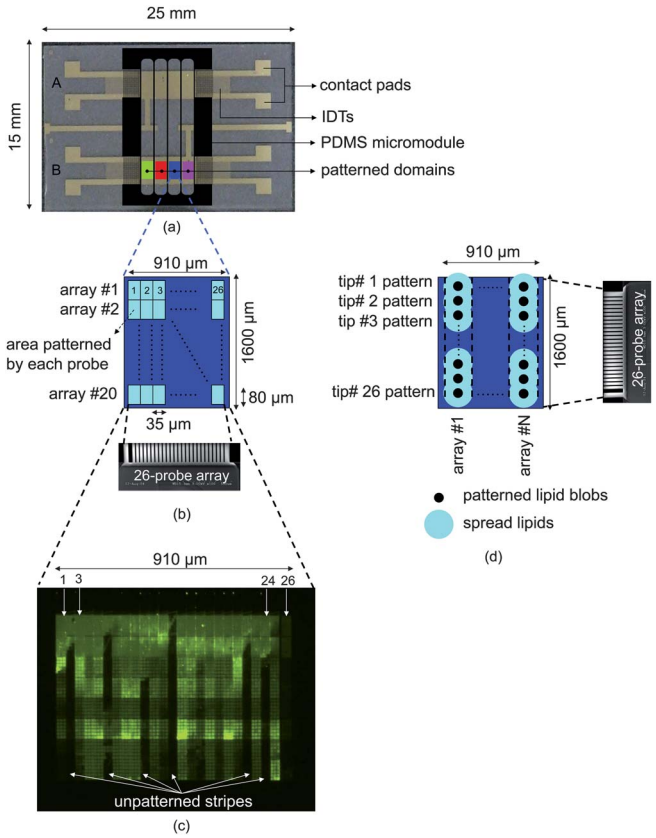

Fig. 1 (a) Real image of a dual-SAW-device biochip with the "footprint" of the four microfluidic channels (CAD design appearing in black colour) and the formed domains. One of the two devices was used for the experiments. (b) Zoomed domain with a schematic of the direct-write concept for filling the area with small lipid rectangles using the 26-probe array; each probe patterns one small rectangle. (c) Fluorescence microscopy image (4×) of biotin lipids patterned *via* the direct-write concept, resulting in sharp side edges but also in empty patches and non-uniform overall pattern. (d) The patterning approach based on spreading of lipid blobs; the dashed lines indicate the uniform pattern upon merging of the spread blobs.

more efficient multiplicity. Surface patterning techniques such as micro-contact printing,[11,12] inkjet spotting,[13] lithography-related techniques[14] and other emerging methods[15,16] are already used for immobilization of biomolecules on a substrate in patterns of various shapes and sizes; different molecules can, thus, be patterned with high accuracy, spatial resolution and multiplexity, promoting the multi-sample analysis.

In the present work surface patterning was achieved by means of Dip-Pen Nanolithography (DPN), a technique that uses a molecular ink coated Scanning Probe Microscope (SPM) tip to directly deposit materials on a surface with lateral resolution well below 100 nm.[17–19] DPN operates under ambient conditions, and has even been demonstrated under water,[20] which is extremely advantageous for biomolecular patterning as it does not require harsh environments like vacuum, UV radiation or wet chemicals.

Being a direct-write method, DPN permits the drawing of arbitrary patterns at will, unlike photolithography-based techniques and micro-contact printing, which are less flexible and versatile since a mask is required. Importantly, DPN is advantageous over other types of patterning methods as it is a constructive printing method where many different chemical functionalities can be integrated onto a single surface without the risk of feature cross-contamination induced by selective adsorption methods. Moreover, for large-scale patterns, like those required in this work, DPN carried out in parallel with arrays of cantilevers over centimetre length scales accelerates the patterning step surpassing the alleged "slowness" of direct writing.[21,22]

The DPN process has been demonstrated for a variety of inks (self-assembled monolayers, DNA, proteins, *etc.*, with sub-100 nm resolution[23,24]) and substrates (silicon, glass, metals, polymers, *etc.*). Lipids are particularly well suited for parallel and multiplexed DPN on a variety of different surfaces.[21,25] DPN has been used in specific interaction studies,[26] in the investigation of a material's suitability for biocompatible/mimetic applications and cell–substrate interactions,[25] in the fabrication of nanoscale biomolecular arrays[27] and complex multi-functional (nano) structures,[28] as well as in lab-on-a-chip applications.[29] In all cases, however, DPN has been utilized on wafer pieces or slides of arbitrary size, but never for direct patterning of a ready-to-use biosensor chip that imposes specific pattern features based on the biosensor operational requirements, like in our case.[30] On the other hand, SAW devices have never been subjected to biomolecule patterning before, especially *via* DPN. Moreover, all DPN demonstrations to date aim at the minimization of the pattern size towards nanoscale features, but hardly any references exist targeting spatially continuous (*i.e.*, not spot-like) hundred-micron-sized patterns, tailor-made for specific purposes and under particular geometrical restrictions.

To demonstrate the convergence of DPN and SAW devices, and particularly in the multi-analyte configuration facilitated through the μF-on-SAW, various lipid types were used as inks for DPN. Lipids were chosen based on the availability of various functional head groups, which allows for patterning of several different receptors. Moreover, lipids are the basis of biological membranes and they can simulate the cell membrane, with the proper integration of other functional species such as membrane proteins. The selection of the patterning strategy and the optimization of the procedure to achieve compatibility with the μF-on-SAW requirements are discussed. The patterned lipids with the different functional head groups and the interactions with their specifically bound molecules were monitored with the μF-on-SAW platform and fluorescence microscope, verifying in both ways the efficiency of DPN patterning at the micro-scale and the functionality of the head groups. Achieving the reduction of the device preparation steps, this proof-of-principle of merging DPN with the μF-on-SAW is promising for the development of a competitive, integrated, multi-analyte detection platform.

Experimental

Multi-analyte acoustic microsystem

The biosensing component of the microsystem comprises a dual SAW device biochip based on a quartz piezoelectric substrate that supports the acoustic wave. The rotated *Y*-cut (42.5°) *z*-propagating crystal allows shear horizontal wave polarization,

rendering the device suitable for liquid-based sensing applications. Two sets of Au interdigital transducers (IDTs) are photolithographically patterned at the two edges of the substrate with an Au layer between the two sets. The Au is deposited to prevent acoustoelectric interactions (Au thin film thickness is 100 nm with a 20 nm thick intermediate Cr adhesion layer). The overlap between the IDT fingers (acoustic aperture) is 1.6 mm and defines the width of the active sensing area; a polymethylmethacrylate (PMMA) layer, covering both IDT sets and the sensing area, was spin-coated (P6700, Specialty Coating Systems Inc.) on top of the sensor for sensitivity enhancement[31] leading to the Love wave mode configuration.[32] A 14% ($g_{PMMA}/g_{solvent}$) solution in 2-ethoxyethyl acetate (>99%, Aldrich) was used, followed by thermal treatment for solidification (180 °C for 2 h). Operational features of the devices are: IDT periodicity 32 μm; frequency 155 MHz; PMMA thickness 0.70 μm; penetration depth ~50 nm within the sensing medium.

The fluidic component of the microsystem comprises a four-parallel-channel microfluidic module, made of polydimethylsiloxane (PDMS, Dow Corning Corp.) by means of rapid prototyping and replica molding (soft lithography[33]). The microchannels cross the acoustic propagation path (device's long axis) perpendicularly upon assembly on the biochip, giving rise to four distinct sub-area domains (Fig. 1(a)) with 1.76 mm^2 surface area each. More details on the design considerations and limitations can be found in previous work.[7] The biochip and micromodule are reversibly assembled *via* mild pressure so as to achieve reusability of the platform. The PMMA layer was dissolved in acetone after each experiment and a new layer was spin-coated prior to reuse.

Measurement principle and instrumentation

The IDT electrodes transform the input electric signal into a propagating acoustic wave, and back to an electric output signal, owing to the piezoelectric effect. Any process taking place on the sensor surface causes a change in the phase (ΔPh) and amplitude (ΔA) of the acoustic wave.[34] In biomolecular interactions (surface adsorption, specific binding, *etc.*) ΔPh is mainly related to the amount of bound mass, whereas ΔA to viscosity changes in the sensing medium.[35] Although both parameters are often needed for sophisticated acoustic measurements (such as investigation of molecular conformation changes[36–38] and/or biofilm viscoelasticity/complex shear modulus evaluation[39,40]) only ΔPh is probed in this work in order to verify the quality of the patterning and functionality of the patterned species through specific binding. A network analyzer was implemented for the acoustic measurements allowing the real-time monitoring of the interactions with data acquisition every 14 s. A syringe pump was used to provide steady flow at 5 μL min^{-1}. The microchannels were used in a serial, instead of simultaneous, manner in order to avoid signal interference.[7]

DPN patterning platform

The DPN patterning was carried out with a commercially available DPN 5000 system (Nscriptor, NanoInk Inc., USA). The temperature and humidity of the chamber were constantly monitored and were rapidly changed and reset by the user according to the desired application.

A one-dimensional array of 26 cantilevers (Fig. 1(b)) was used for the patterning (type F multi-probe array A-26, NanoInk Inc.). The scan range of the piezo was 80 × 80 μm, and the distance between neighbouring tips was 35 μm, so that an area of 910 × 80 μm was patterned using the piezo actuator. For further patterning the probe array was removed from the surface, forwarded to another initial spot and approached again. The actuation of the cantilever array was followed on screen by means of a camera. The coordinates of the initial patterning point as well as the "route" of the probe array were preset by the user in the software so that the entire patterning procedure was automated. The final optimized procedure is described in Results and discussion as the patterning conditions, dimensions and methodology were part of the actual investigation process.

Ink wells of type W4 and IWL-0021-01 (NanoInk Inc.) were used and filled with a chloroform solution of the phospholipid ink (1 mL, 10 mM, doped with 1 mol% of the dye-labeled lipid in the case of doped inks). The solvent was allowed to evaporate for at least 1 h in vacuum (50 mbar) before dipping the tips in the ink wells; the latter were then stored in a desiccator chamber (25% humidity). All probes of the array were dipped into the same ink well for their functionalization and four different probe arrays were used.

DPN fluorescence microscopy

An inverted TE 2000 fluorescence microscope (Nikon) was used. Green (FITC) and red (Texas Red) filters were used for the fluorescence. The exposure times were kept as low as possible (a few seconds) to avoid bleaching. The microscope was also used for the inspection of the tip array intactness prior to every patterning procedure, as well as for the precise mounting of the microfluidic module on the biochip prior to the acoustic experiments (taking into consideration a ±100 μm placement error due to manual alignment).

Biomolecules

The lipids used in this work were purchased from Avanti Polar Lipids, USA: (i) DOPC (1,2-dioleoyl-*sn-glycero*-3-phosphocholine); (ii) DOGS-NTA-Ni {1,2-dioleoyl-*sn-glycero*-3-[(*N*-(5-amino-1-carboxypentyl)iminodiacetic acid)succinyl] (nickel salt)}; (iii) biotinylated phospholipid (1,2-dipalmitoyl-*sn-glycero*-3-phosphoethanolamine-*N*-(cap biotinyl) (sodium salt)); and (iv) dinitrophenyl (DNP)–lipid (16 : 0 DNP Cap PE antigenic lipid {1,2-dipalmitoyl-*sn-glycero*-3-phosphoethanolamine-*N*-[6-[(2,4-dinitrophenyl)amino] hexanoyl] (ammonium salt)}).

Fluorescent lipids: (i) rhodamine lipid [2-dioleoyl-*sn-glycero*-3-phosphoethanolamine-*N*-(lissamine rhodamine B sulfonyl) (18 : 1 lissamine rhodamine/PE)] and (ii) fluorescein lipid [1,2-dioleoyl-sn-*glycero*-3-phosphoethanolamine-*N*-(carboxyfluorescein) (ammonium salt)].

Monoclonal anti-DNP IgE antibody (SPE-7) was purchased from Sigma-Aldrich, Germany. Histidine-tagged green fluorescent protein (his-GFP) was provided by N. Theilacker, Dr M. Franzreb, Institute for Chemical Technology, KIT.[25] Fluorescently labeled (Cy3 dye), streptavidin and bovine serum albumin (BSA) were purchased from Sigma-Aldrich.

All solutions were prepared in phosphate buffered saline (PBS, Invitrogen) at pH 7.4, and the washing buffer was the same.

Results and discussion

Establishment of the DPN patterning methodology on μF-on-SAW; process characteristics

The design of the multi-analyte acoustic microsystem imposes some operational and geometrical limitations to the patterning procedure. At first, the acoustic wave is a plane wave, so it is desirable that it propagates through patterned species with line-edged borders parallel to the wavefronts.[7] If the patterns' borders are of arbitrary shape it is highly likely that the wavefronts will be distorted (diffracted) and the output signal will not be representative of the surface processes. It should also be taken into consideration that each sensor domain (defined by the microfluidic channels) covers a surface area (1.76 mm^2) much larger than the tip array can pattern in a single step (0.073 mm^2). Therefore, it is impossible to achieve the desired pattern within each rectangular domain with a single pass of the probe array, but only through sequential steps (*i.e.*, detach and re-approach). As the desired domain width is covered by the total writing width (910 μm) of the array, the latter does not need to be shifted laterally. On the other hand, as the array patterns 80 μm in the forward direction it has to be moved 20 times in order to complete the 1600 μm required (Fig. 1(b)).

The result of these DPN steps reveals a patterned domain with indeed sharp edges at the borders (Fig. 1(c)). Sharp edges are desirable for SAW sensors in order to minimize scattering of acoustic waves at the edges, and would be difficult to achieve with other microarray methods such as inkjet printing or micro-pin spotters.[41] This procedure, though, is quite time-consuming because of the many small rectangles that should be added to complete the sub-area domain. Indicatively, approximately 10 min were required for an 80 × 910 μm^2 pattern area (at 5 μm^2 s^{-1} average writing speed), while approximately three hours for one domain (without accounting for the time needed to frequently re-dip the tips in the ink wells due to the ink consumption and gradual decrease of pattern quality). Even though this procedure could in principle be accomplished in an automated way, it would still require a long time for the complete patterning of a domain, not to mention the entire sensor surface. Moreover, in the case of insufficient inking or misalignment of one or more probes, the above approach would be reflected on the pattern as one or more missing lipid stripes (Fig. 1(c)), which would have severe impact on the uniformity of the pattern and the wave propagation.

An alternative approach is based on the experimentally verified observation that, under particular humidity conditions, patterned lipids exhibit a rather fluidic behaviour and spread laterally on the surface to form supported lipid bilayers when hydrated on hydrophilic surfaces.[21,25,42,43] This spreading effect is further enhanced by the non-covalent but physisorptive interaction between the lipids and the surface. Thus, a large lipid spot or "blob" for example can spread into a circular-shape, single- or multi-stack bilayer structure if the proper humidity conditions exist (there is usually a distribution of single- and multi-layer lipids, depending on the humidity and writing speed conditions[21]). Following this approach, one entire sensor domain (Fig. 1(a)) was patterned within only 10 min as the detach–redip–reapproach procedure was repeated far less times than the previous option (two to six times, depending on the lipid case, see the following section for details). In addition, closely patterned blobs (as close as neighbouring tips allow) can spread enough as to merge and eventually form a uniform structure with linear, sharp edges parallel to the wavefront (Fig. 1(d)). In the present approach the lipid blob array was patterned in the same direction as the microchannel axis. If necessary for practicality in manufacturing, this approach could be carried out using parallel DPN arrays.[21,22]

Patterning design and conditions

In order to pattern multiple species, the optimum patterning conditions (*e.g.*, dipping and inking time, number of lipid blobs, *etc.*) were investigated for four different lipids: (i) a mixture of DOPC with DNP-lipids (10 mol%, doped with rhodamine); (ii) a mixture of DOPC with DOGS-NTA-Ni lipids (30 mol%, doped with fluorescein); (iii) a mixture of DOPC with biotin-lipids (4 mol%, doped with fluorescein) and (iv) fluorescein-labeled DOPC for control acoustic experiments. The optimum amount of each kind of functional lipids mixed with the DOPC carrier was defined as the mol% at which saturation of the fluorescent signal of the bound biomolecule occurred.[25]

For the inking process, humidity is a key factor to efficient tip coating with lipids.[21] At 70% relative humidity lipids behave like liquid crystals and can coat tips once in contact with the ink well. For the first dipping, the tips were left for 25–30 min in contact with the ink, whereas the subsequent re-dippings lasted 5–7 min for DNP lipids, biotin-lipids and DOPC, and 10 min for NTA-Ni lipids, all taking place at 70% humidity. Right after inking the probes could write a uniform array of spots (or "blobs"). The writing duration (*i.e.*, the contact time between the tip and the surface) did not vary much within the different types: 5 s for the DNP lipids and DOPC, 10 s for biotin lipids, and 15–20 s for NTA-Ni lipids, which is tremendously faster than the time required during the initial, direct-write patterning approach. This resulted in an overall printing time of 10 min (including the redip steps) for each domain.

For lipid patterning itself, the general applicability of lipid spreading has been shown in previous work.[21,25] Each lipid type exhibits its maximum spreading at different humidity conditions, which also depends on the lipid chemistry and the used substrate. The latter is the same surface (PMMA) for all cases in our work but the chemistry of the lipids differs, so ideally each lipid type needs to be stored at different humidity conditions to achieve its maximum spreading. This, however, is impossible since all different lipids are patterned on the same device, which is then stored at specific humidity conditions (overnight in desiccator at 25% humidity) so in principle they will not spread the same. Therefore, an investigation of the extent of spreading under the given storage humidity conditions was carried out and consequently a definition of the proper pattern design for each lipid type (*i.e.*, how many arrays and how big spacing between them) so that they all result in uniform, 900–1000 μm wide structures.

A single array from each lipid type was initially patterned on PMMA in order to investigate the extent of spreading. After

overnight storage in the desiccator the spreading was symmetrical on both sides of the initial array; the following values represent the spread pattern width (Fig. 2): (i) 950 ± 50 μm for the DNP-lipids, (ii) 330 ± 30 μm for the NTA-Ni lipids, (iii) 580 ± 50 μm for the biotin lipids and (iv) 1050 ± 50 μm for the DOPC lipids. The dimensions were measured under the fluorescence microscope with 4× magnification and the average values and standard deviations derived from at least four patterns of the same lipid type. Based on these findings it was possible to optimize the distance between adjacent pattern arrays, considering that: (i) the width of the spread pattern(s) should be such that neighbouring different lipid types do not overlap (*i.e.*, each lipid type should not exceed the width of its corresponding domain after spreading), and (ii) there should be no gap between spread patterns of the same lipid type within the domain; on the contrary, overlapping is acceptable. Conclusively, the pattern of the entire SAW device included fourteen arrays all together (the following seven in duplicates symmetrically above and below the device horizontal axis) so that the entire 1600 μm acoustic aperture is covered with spread lipids: one DNP-lipid array in μF4; three NTA-Ni-lipid arrays 300 μm apart in μF3; two biotin-lipid arrays 300–350 μm apart in μF2; one DOPC array in μF1 (Fig. 2).

Acoustic experiments

Once the patterned acoustic biochip was removed from the desiccator, the microfluidic module was assembled on it under microscope inspection. The biosensing experiments included the following injections (Fig. 3(a)): (i) PBS for rinsing excessive lipid

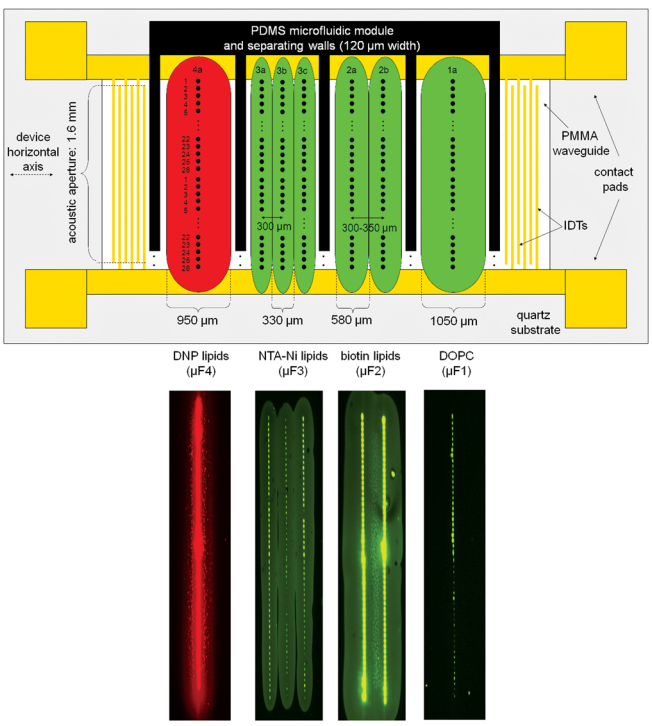

Fig. 2 Top: schematic of the design and arrangement of the four different lipid arrays on the sensor. Bottom: fluorescent microscope images (4× magnification) of the four patterned lipid types at the domains corresponding to the schematic of the top figure.

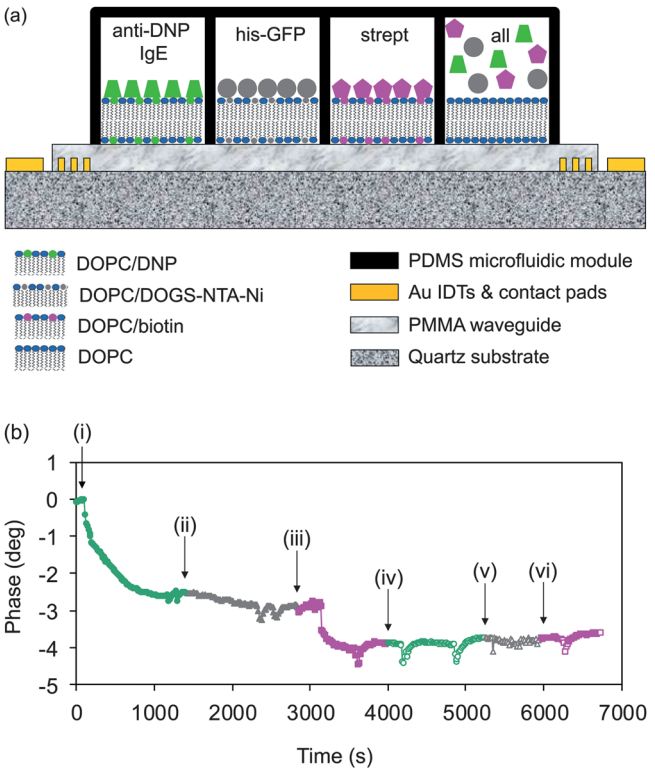

Fig. 3 (a) Schematic distribution of the patterned lipids and their corresponding biomolecule analytes in the four sensor domains. (b) Acoustic sensogram of the probed interactions between the patterned functionalized lipids with their corresponding biomolecule analytes: (i) anti-DNP IgE on DNP lipids, (ii) his-GFP on NTA-Ni lipids, (iii) streptavidin on biotin lipids, (iv) anti-DNP IgE on DOPC, (v) his-GFP on DOPC and (vi) streptavidin on DOPC. The concentrations in all cases were 100 μg mL^{-1}. BSA blocking and PBS rinsing steps are not marked for simplicity reasons. Some signal spikes are due to the syringe pump.

multilayers until stabilization of the acoustic signal, (ii) BSA (1 mg mL^{-1}) as a blocking agent to prevent non-specific interactions of analytes and fill possible gaps (non-patterned regions) on the biosensor domain, followed by PBS wash step and (iii) analyte binding (100 μg mL^{-1}), followed by a PBS wash step. This procedure was repeated in all microchannels in a sequential way for the following analytes: anti-DNP IgE in μF4, interacting with DOPC/DNP lipids *via* an antibody–antigen-like interaction; his-tagged GFP in μF3, interacting with patterned DOPC/DOGS–NTA–Ni lipids *via* the histidine residues that bind a bivalent cation (*e.g.*, Ni^{2+}) complexed with an *N*-nitrilotriacetate (NTA);[44] streptavidin in μF2, interacting with patterned DOPC/biotin lipids *via* biotin–avidin bond; all three mentioned proteins sequentially in μF1, interacting with pure DOPC as control experiments. The acoustic response appears in the sensogram of Fig. 3(b), where only the specific interaction (and control) steps appear for simplicity reasons (the BSA-blocking steps have been omitted). In previous experimental procedures with the μF-on-SAW where the receptor adsorption was accomplished *in situ* in a flow-through manner, the experimental time was longer by at least 30 min per microchannel,[9] *i.e.*, at least 2 h for the entire biochip. This duration was even longer when two-step immobilization was needed, namely, protein

G and antibody, for the subsequent specific binding of cardiac markers.[10]

The interactions of anti-DNP IgE with DNP-lipids and streptavidin with biotin-lipids were clearly detected ($\Delta Ph_{IgE} = 2.5 \pm 0.3$ deg, $\Delta Ph_{strept} = 1.2 \pm 0.2$ deg), whereas the his-GFP interaction with NTA-Ni lipids was slightly above the detection limit of the sensor ($\Delta Ph_{his\text{-}GFP} = 0.3 \pm 0.2$ deg). Indicatively for the streptavidin interaction, Fig. 4(a–c) shows the fluorescent images of the patterned biotin-lipids (green), the bound streptavidin (red) and their overlap as a verification of the interaction. Control experiments were carried out in μF1 where DOPC with no functional groups was patterned. No phase change was detected after injection of anti-DNP IgE antibody, streptavidin, or his-GFP, implying negligible non-specific binding between the analytes and the lipids without functional head groups.

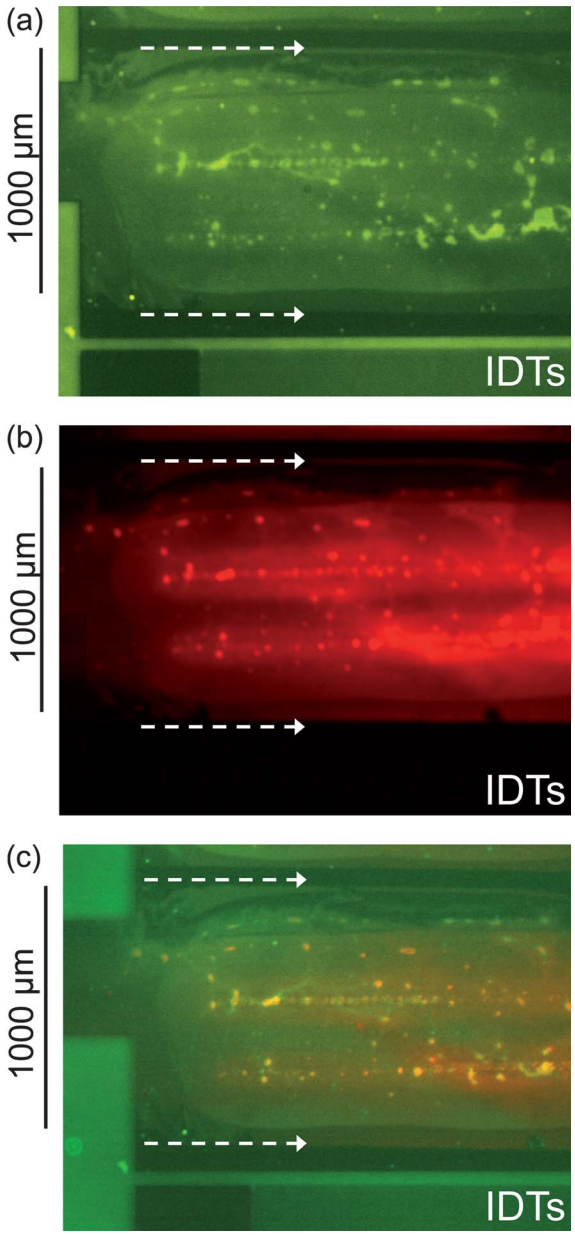

Fig. 4 Fluorescent microscope images of streptavidin (100 μg mL^{-1}) binding to patterned biotin lipids on the acoustic sensor: (a) biotin-lipids, (b) streptavidin and (c) overlay of (a) and (b). In all cases the images were taken at 4× magnification and the dashed lines indicate the borders of the area domain on the sensor, as defined by the microchannel walls.

To understand the low acoustic signal observed during his-GFP binding to NTA-Ni lipids on the biochip, the interaction was additionally investigated off-biochip, with green fluorescent labeled his-GFP binding to non-labeled NTA-Ni lipids (the latter being non-labeled prevents overlap with the green-labeled his-GFP); the fluorescence microscope images verified the efficient binding (data not shown). Based on previous work where NeutrAvidin (neu) adsorbed on a 20 nm sputter-coated Au layer on PMMA, it was noticed that the Au film acts as an additional waveguiding medium and enhances sensitivity by two-fold.[45] In the present work the Au layer was not used in order to avoid quenching of the fluorescent dyes. Based on the above, the barely detectable signal of the his-GFP interaction with NTA-Ni lipids is primarily attributed to the lack of the Au layer (note that fluorescence microscopy was used here only as a means of quality control of the patterned lipids, thus, it is in principle not necessary for the acoustic experiments; the Au film will be used in the future without raising any issue). Besides, in previous studies employing an Au layer, biotinylated molecules of the same molecular weight as his-GFP biotinylated protein G (~30 kDa) were clearly detected by the same μF-on-SAW configuration ($\Delta Ph = 1.0$ deg) upon specific binding to NeutrAvidin.[9] This observation also suggests that the weaker interaction between his-tagged proteins and NTA-Ni lipids compared to the avidin–biotin interaction[44] can also affect the acoustic signal and justify the observed poor response.

To assess the sensitivity of the DPN-patterned μF-on-SAW setup, the current results are compared with previous acoustic experimental work where streptavidin specifically interacted with biotinylated lipids deposited on the Au surface through vesicle fusion, a commonly used method for modifying surfaces with lipid bilayers.[46] Experiments carried out on a standard SAW configuration utilizing the total surface area modified with biotin-lipids through vesicle fusion showed that a full-coverage streptavidin layer resulted in $\Delta Ph = 1.4 \pm 0.1$ deg. Comparison of the ΔPh absolute values and suitable normalization concerning (i) sensitivity differences between the implemented sensors (Au layer, operating frequency), and (ii) surface area differences between the total area of the standard configuration and the sub-area domains of the μF-on-SAW clearly indicate that, apart from the faster analysis procedure that was established, a 5-fold sensitivity increase of the DPN-patterned μF-on-SAW setup was achieved in comparison with the vesicle-fusion lipid deposition and the standard acoustic configuration used.

Conclusions

The present work is the first demonstration of multiplexed patterning of an acoustic device with DPN for multi-sample measurements. Compatibility issues between the patterning method and the μF-on-SAW microsystem were investigated as there are only a few reports on DPN being implemented on a ready-to-use biosensor platform. Four lipid types with different functional head groups (including control) were uniformly patterned on discrete domains of a single acoustic sensor by means of lipid blob arrays exploiting their spreading properties

under suitable humidity conditions. The specific interaction between the patterned lipids' head groups with target analytes was successfully detected by the μF-on-SAW acoustic platform, saving at least 2 h of experimental time due to less on-chip experimental steps compared with *in situ* lipid deposition in a flow-through manner. As for the sensitivity, it is better by at least 5-fold when compared with normalized results derived by the authors in the past under lipid vesicle fusion, and can be further increased when the optimum SAW device configuration is used. The proof-of-principle of this approach renders the μF-on-SAW configuration much more competitive compared to existing technologies and opens the way for its direct utilization in the micro-analytical field since, with the pre-patterning of the capturing species, the actual analyte detection can now be accomplished in a single step. Together with the label-free nature of acoustic sensors, this platform combined with DPN can potentially be developed into a competitive diagnostic tool.

Acknowledgements

This work was partly carried out with the support of the Karlsruhe Nano Micro Facility (KNMF, www.kit.edu/knmf), a Helmholtz Research Infrastructure at Karlsruhe Institute of Technology (KIT, www.kit.edu). K. Mitsakakis wishes to acknowledge the Deutscher Akademischer Austausch Dienst (DAAD) and the Public Benefit Foundation "Alexander S. Onasis" for financial support, and T. Laue from INT, KIT, for training in the DPN facility. K. Mitsakakis and E. Gizeli also thank Dr B.E. Rapp from the IMT, KIT, for their technical support.

References

1 R. McKendry, J. Zhang, Y. Arntz, T. Strunz, M. Hegner, H. P. Lang, M. K. Baller, U. Certa, E. Meyer, H.-J. Güntherodt and Ch. Gerber, *Proc. Natl. Acad. Sci. U. S. A.*, 2002, **99**, 9783–9788.
2 H.-B. Pyo, Y.-B. Shin, M.-G. Kim and H. C. Yoon, *Langmuir*, 2005, **21**, 166–171.
3 J. Wu, F. Yan, J. Tang, C. Zhai and H. Ju, *Clin. Chem.*, 2007, **53**(8), 1495–1502.
4 B. E. Rapp, B. Schickling, J. Prokop, V. Piotter, M. Rapp and K. Länge, *Biomed. Microdevices*, 2011, **13**, 909–922.
5 M. Perpeet, S. Glass, T. Gronewold, A. Kiwitz, A. Malavé, I. Stoyanov, M. Tewes and E. Quandt, *Anal. Lett.*, 2006, **39**, 1747–1757.
6 Y. Luo, M. Chen, Q. Wen, M. Zhao, B. Zhang, X. Li, F. Wang, Q. Huang, C. Yao, T. Jiang, G. Cai and W. Fu, *Clin. Chem.*, 2006, **52**, 2273–2280.
7 K. Mitsakakis, A. Tserepi and E. Gizeli, *J. Microelectromech. Syst.*, 2008, **17**(4), 1010–1019.
8 K. Mitsakakis, A. Tserepi and E. Gizeli, *Microelectron. Eng.*, 2009, **86**, 1416–1418.
9 K. Mitsakakis and E. Gizeli, *Biosens. Bioelectron.*, 2011, **26**, 4579–4584.
10 K. Mitsakakis and E. Gizeli, *Anal. Chim. Acta*, 2011, **699**, 1–5.
11 J. L. Wilbur, A. Kumar, E. Kim and G. M. Whitesides, *Adv. Mater.*, 1994, **6**, 600–604.
12 A. Bernard, J. P. Renault, B. Michel, H. R. Bosshard and E. Delamarche, *Adv. Mater.*, 2000, **12**, 1067–1070.
13 A. Bietsch, J. Zhang, M. Hegner, H. P. Lang and Ch. Gerber, *Nanotechnology*, 2004, **15**, 873–880.
14 P. S. Petrou, M. Chatzichristidi, A. M. Douvas, P. Argitis, K. Misiakos and S. E. Kakabakos, *Biosens. Bioelectron.*, 2007, **22**, 1994–2002.
15 P. Bayiati, A. Malainou, E. Matrozos, A. Tserepi, P. S. Petrou, S. E. Kakabakos and E. Gogolides, *Biosens. Bioelectron.*, 2009, **24**, 2979–2984.
16 T. Drakakis, G. Papadakis, K. Sambani, G. Filippidis, S. Georgiou, E. Gizeli, C. Fotakis and M. Farsari, *Appl. Phys. Lett.*, 2006, **89**(1), 144108.
17 R. D. Piner, J. Zhu, F. Xu, S. H. Hong and C. A. Mirkin, *Science*, 1999, **283**, 661–663.
18 K. Salaita, Y. H. Wang and C. A. Mirkin, *Nat. Nanotechnol.*, 2007, **2**, 145–155.
19 S. Lenhert, H. Fuchs and C. A. Mirkin, in *Nanoprobes*, ed. H. Fuchs, Wiley-VCH, Weinheim, 2009, vol. 6, pp. 171–196.
20 S. Lenhert, C. A. Mirkin and H. Fuchs, *Scanning*, 2010, **31**, 1–9.
21 S. Lenhert, P. Sun, Y. Wang, H. Fuchs and C. A. Mirkin, *Small*, 2007, **3**(1), 71–75.
22 E. J. Irvine, A. Hernandez-Santana, K. Faulds and D. Graham, *Analyst*, 2011, **136**, 2925–2930.
23 K. B. Lee, J. H. Lim and C. A. Mirkin, *J. Am. Chem. Soc.*, 2003, **125**, 5588–5589.
24 L. M. Demers, D. S. Ginger, S. J. Park, Z. Li, S. W. Chung and C. A. Mirkin, *Science*, 2002, **296**, 1836–1838.
25 S. Sekula, J. Fuchs, S. Weg-Remers, P. Nagel, S. Schuppler, J. Fragala, N. Theilacker, M. Franzreb, C. Wingren, P. Ellmark, C. A. K. Borrebaeck, C. A. Mirkin, H. Fuchs and S. Lenhert, *Small*, 2008, **4**, 1785–1793.
26 K. B. Lee, E. Y. Kim, C. A. Mirkin and S. M. Wolinsky, *Nano Lett.*, 2004, **4**, 1869–1872.
27 J. H. Lim, D. S. Ginger, K. B. Lee, J. Heo, J. M. Nam and C. A. Mirkin, *Angew. Chem., Int. Ed.*, 2003, **42**, 2309–2312.
28 S. Lenhert, F. Brinkmann, T. Laue, S. Walheim, C. Vannahme, S. Klinkhammer, M. Xu, S. Sekula, T. Mappes, T. Schimmel and H. Fuchs, *Nat. Nanotechnol.*, 2010, **5**, 275–279.
29 C. Vannahme, S. Klinkhammer, F. Brinkmann, S. Lenhert, T. Grossmann, U. Lemmer and T. Mappes, in *Proceedings of SPIE*, 2010, vol. 7715, pp. 77151H–77151–77110.
30 P. M. Mendes, C. L. Yeung and J. A. Preece, *Nanoscale Res. Lett.*, 2007, **2**, 373–384.
31 A. Rasmusson and E. Gizeli, *J. Appl. Phys.*, 2001, **90**, 5911–5914.
32 E. Gizeli, *Anal. Chem.*, 2000, **72**, 5967–5972.
33 J. C. McDonald, D. C. Duffy, J. R. Anderson, D. T. Chiu, H. Wu, O. J. A. Schueller and G. M. Whitesides, *Electrophoresis*, 2000, **21**(1), 27–40.
34 D. S. Ballantine, R. M. White, S. J. Martin, A. J. Ricco, E. T. Zellers, G. C. Frye and H. Wohltjen, in *Acoustic Wave Sensors*, Academic Press, San Diego, CA., 1997.
35 S. J. Martin, G. C. Frye and S. D. Senturia, *Anal. Chem.*, 1994, **66**, 2201–2219.
36 G. Papadakis, A. Tsortos and E. Gizeli, *Nano Lett.*, 2010, **10**(12), 5093–5097.
37 A. Tsortos, G. Papadakis and E. Gizeli, *Biosens. Bioelectron.*, 2008, **24**, 836–841.
38 G. Papadakis, A. Tsortos, K. Mitsakakis and E. Gizeli, *FEBS Lett.*, 2010, **584**, 935–940.
39 M. V. Voinova, M. Rodahl, M. Jonson and B. Kasemo, *Phys. Scr.*, 1999, **59**, 391–396.
40 M. Weiss, W. Welsch, M. v. Schickfus and S. Hunklinger, *Anal. Chem.*, 1998, **70**, 2881–2887.
41 Y. Fang, *J. Am. Chem. Soc.*, 2006, **128**, 3158–3159.
42 J. Nissen, S. Gritsch, G. Wiegand and J. O. Radler, *Eur. Phys. J. B*, 1999, **10**, 335–344.
43 B. Sanii and A. N. Parikh, *Soft Matter*, 2007, **3**, 974–977.
44 E. Gizeli and J. Glad, *Anal. Chem.*, 2004, **76**, 3995–4001.
45 K. Mitsakakis, A. Tsortos, J. Kondoh and E. Gizeli, *Sensor Actuator. B Chem.*, 2009, **138**, 408–416.
46 E. Gizeli, M. Liley, C. R. Lowe and H. Vogel, *Anal. Chem.*, 1997, **69**, 4808–4813.

